

Phys. Chem. Res., Vol. 4, No. 4, 627-641, December 2016

DOI: 10.22036/pcr.2016.16429

A Theoretical Study of Nonlinear Optical Features of Alumina Nanostructures with the Groups III and VI Dopants

M. Solimannejad

Department of Chemistry, Faculty of Science, Arak University, Arak 38156-8-8349, Iran

(Received 2 May 2016, Accepted 1 July 2016)

A comprehensive study on the structural, electronic and nonlinear optical (NLO) properties of alumina nanostructures (Al_2O_3)_n with n = 2-5 belonging to the groups III and VI dopants carried out by density functional theory. The NBO charges exhibit dopant atoms caused to the increasing charge transfer and introduces acceptor-donor model for NLO response of alumina nanostructures. Under the influence of doping S and Se, the energy gap decreases, because high energy level is formed as the new HOMO orbitals in the primary gap of pristine nanostructures. Furthermore, the results of the present study show that dopant atoms enhance NLO response in the alumina nanostructures and the greatest values are obtained for α , β_0 and γ_{tot} through doping Se in $\text{Al}_{10}\text{O}_{15}$.

Keywords: Nonlinear optics, Alumina, Hyperpolarizability

INTRODUCTION

The fabrication of nanoscale-structure materials is considered for applications in new electric, magnetic and optical devices [1]. Tubular or spherical nanoparticles of multiple inorganic compounds with different stoichiometries have been previously synthesized [2,3]. These contain, for example, nanotubes of boron nitride (1:1 stoichiometry) [4], silica (1:2) [5], and alumina (2:3) [6]. Chemical and physical properties of these new materials are also dependent on the shape and size of the nanostructures. In recent years, molecular structures of alumina (Al_2O_3) nanotubes have been synthesized [7]. Alumina is the most significant ceramic material that has widespread technological use such as electronics, optics, biomedical, and mechanical engineering to catalyst support. The importance of these materials is mainly due to their external hardness, high melting point, and low electrical conductivity [8-10]. In recent years, aluminum oxide clusters have been extensively studied experimentally [11,12] and

theoretically [13-20] as well; mainly due to their importance in understanding the different properties of ceramic materials.

The (Al_2O_3)₂₋₅ cages are lower in energy than other isomers and might exist under normal conditions [19,20]. For (Al_2O_3)₆₋₁₀, the cage-dimer structures are shown to be more stable than the corresponding cage structures. Thus, the (Al_2O_3)₅ cages would be the largest cage as a global minimum. This is the reason for our motivation to focus on cluster with n = 2-5 in the present study.

Nonlinear optical (NLO) materials research has progressed surprisingly over the last four decades [21]. An appreciable attempt has been made for discovery high-performance NLO materials [22-27]. To the present time, many approaches have been suggested to increase the NLO response of materials, including the use of molecules with extended π -electron systems, twisted π -electron systems, octupolar molecules, enhanced push-pull effects, bond length alternation (BLA) theory, incorporation of ligated metal into the organic compounds [28-33], and the introduction of donor/acceptor groups [34]. Also, excess electron compounds were suggested as new potential high-performance NLO materials [35,36]. Li and co-workers

*Corresponding author. E-mail: m-solimannejad@araku.ac.ir

have made many attractive reports on NLO material with Li-doped electride/salt complexes [37,38]. Moreover, nonlinear optical properties such as hyperpolarizabilities are connected to an enormous classify of physical phenomena with potential applications in future nanostructure technologies where technologically appropriate nanostructures approach the size of atomic clusters [39,40].

In this study, the elements of groups III and VI of the periodic table are considered to be doped in the lowest-energy structures of $(\text{Al}_2\text{O}_3)_n$ with $n = 2-5$. Previous studies have reported the synthesis and experimental study such as vibrational properties and monitoring the intensity of the mass peak of these nanostructures [41,42]. In the present study, alteration of structural, nonlinear optical and electronic properties of these nanostructures with enlargement of nanostructure and location of doping are reported for the first time.

COMPUTATIONAL DETAILS

The geometries of studied alumina nanostructures were fully optimized employing Becke-style 3-parameter [43] of density functional theory (DFT) [44] with the standard 6-31+G(d) basis set. It should be noted that B3LYP is the usual approach for inspecting the nanostructures [45,46]. The harmonic vibrational frequencies were calculated to approve that an optimized geometry properly fits a local minimum that has only real frequencies. The natural bond orbital (NBO) charges [47] were computed at the same level. To appraise the electronic and optical properties, it is necessary to select a proper method. The CAM-B3LYP method has been found to be appropriate for calculating the NLO properties [48,49]. It has been shown that this functional provides good results for electronic excitation energies [48,50,51], first [52], and second hyperpolarizabilities [53]. The standard 6-31+G(d) basis set has been recommended for large molecules [54]. The results of previous studies show that there is a little difference between the results of calculations with the 6-31+G(d) and larger basis sets [55,56]. Therefore, the static first and second hyperpolarizability of alumina nanostructures are evaluated by the finite-field (FF) approach under an electric field magnitude of 0.0001 a.u., at the CAM-B3LYP/6-31+G(d) level in this work. All calculations are carried out

using the Gaussian 09 package [57] with default convergence criteria. The SCF convergence criteria are set to 10^{-8} Hartree on the density (SCF = Tight), while the convergence of geometric optimizations are adjusted to maximum force and root-mean-square (rms) force of 4.5×10^{-4} and 3.0×10^{-4} Hartree. Bohr⁻¹, respectively, and maximum and rms displacements of 1.8×10^{-3} and 1.2×10^{-3} Bohr, respectively.

The energy gap (E_g) value is calculated to study electronic properties of the considered nanostructures. These amounts have the subsequent operational equation:

$$E_g = (\varepsilon_L - \varepsilon_H) \quad (1)$$

where ε_H and ε_L are the highest occupied molecular orbital (HOMO) and the lowest unoccupied molecular orbital (LUMO) energies, respectively.

The total energy of a molecular system in the attendance of a homogeneous electric field can be noted as [58,59],

$$E = E^0 - \mu_i F_i - \frac{1}{2} \alpha_{ij} F_i F_j - \frac{1}{6} \beta_{ijk} F_i F_j F_k - \frac{1}{24} \gamma_{ijkl} F_i F_j F_k F_l \dots \quad (3)$$

where E^0 is the molecular total energy lacking the electric field and F_i is the electric field component along i direction. The μ_i , α_{ij} , β_{ijk} and γ_{ijkl} mark dipole, polarizability, the first hyperpolarizability and the second hyperpolarizability, respectively. The average polarizability (α), first hyperpolarizability (β_0) and second hyperpolarizability (γ_{tot}) are written as:

$$\alpha = \frac{1}{3} (\alpha_{xx} + \alpha_{yy} + \alpha_{zz}) \quad (4)$$

$$\beta_0 = (\beta_x^2 + \beta_y^2 + \beta_z^2)^{1/2} \quad (5)$$

in which

$$\beta_i = \frac{3}{5} (\beta_{iii} + \beta_{iij} + \beta_{ikk}) \quad i, j, k = x, y, z \quad (6)$$

$$\gamma_{tot} + \frac{1}{5} [\gamma_{xxxx} + \gamma_{yyyy} + \gamma_{zzzz} + 2(\gamma_{xxyy} + \gamma_{xxzz} + \gamma_{yyzz})] \quad (7)$$

β_0 is static first hyperpolarizability identified as a second-order nonlinear optical response (NLO) coefficient and γ_{tot} is static second hyperpolarizability known as the third-order nonlinear optical response coefficient [60].

RESULTS AND DISCUSSIONS

Optimized Structure and NLO Response of Alumina Nanostructures

The lowest energy structures for each size of $(\text{Al}_2\text{O}_3)_n$ nanostructures, with $n = 2-5$ and real frequency, have been obtained at the B3LYP/6-31+G(d) level as exhibited in Fig. 1. These nanostructures consist of 6-, 8-, or 10-membered rings with saturated valence states of Al and O atoms on the

surfaces. The bond lengths of Al-O in these nanostructures are listed in Table 1. These results are in good agreement with the previous studies [7,20]. Previous analysis of the atomic structures reveals that the lowest energy structures evolve with 4-membered Al_2O_2 , 6-membered Al_3O_3 , and 8-membered Al_4O_4 rings having alternate Al and O atoms. Among these, there is a preference for 4-membered and 6-membered rings [20].

The electronic and optical properties of these nanostructures are also investigated. The achieved frontier molecular orbital energies (ϵ_H and ϵ_L), and the calculated energy gap (E_g) values for the considered alumina nanostructures are listed in Table 2. The obtained energy gaps for these nanostructures are in the range 4.286-5.177

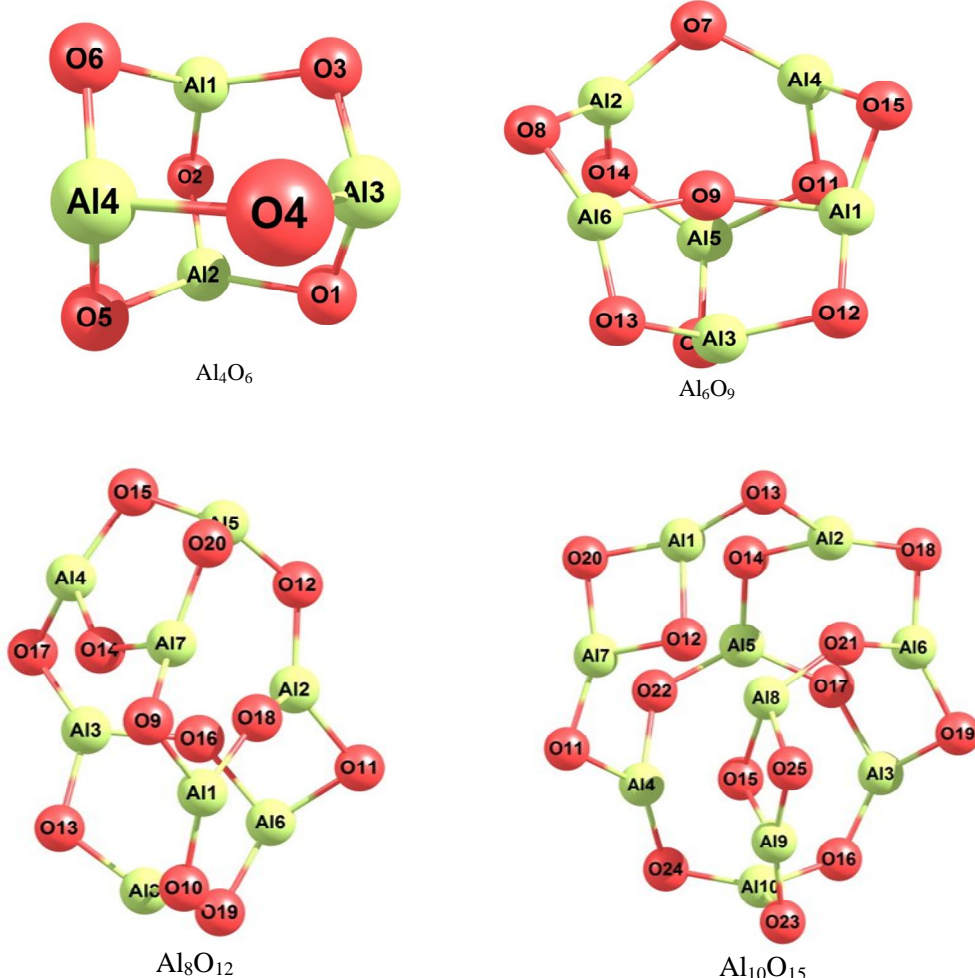


Fig. 1. Geometry of pristine nanostructures.

Table 1. Calculated Equilibrium Bond Lengths (\AA) in Doped Alumina Nanostructure

Compound	Bond length	Compound	Bond length	Compound	Bond length	Compound	Bond length
Al_4O_6		Al_6O_9		Al_8O_{12}		$\text{Al}_{10}\text{O}_{15}$	
Al1-O4	1.744	Al1-O9	1.951	Al1-O9	1.716	Al8-O25	1.782
Al5-O7	1.744	Al6-O9	1.792	Al7-O9	1.766	Al9-O15	1.828
Al5-O6	1.744	Al6-O8	1.714	Al6-O11	1.709	Al9-O23	1.697
				Al6-O16	1.787	Al9-O25	1.704
$\text{Al}_4\text{O}_5\text{S}$		$\text{Al}_6\text{O}_8\text{S}$		$\text{Al}_8\text{O}_{11}\text{S}$		$\text{Al}_{10}\text{O}_{14}\text{S}$	
Al3-S10	2.239	Al1-O8	1.977	Al1-S20	2.163	Al8-S25	2.284
Al3-O7	1.740	Al6-O8	1.802	Al7-S20	2.252	Al9-S25	2.148
Al8-O6	1.742	Al2-S15	2.281	Al6-O10	1.710	Al9-O15	1.815
		Al6-S15	2.162	Al6-O15	1.790	Al9-O23	1.706
$\text{Al}_4\text{O}_5\text{Se}$		$\text{Al}_6\text{O}_8\text{Se}$		$\text{Al}_8\text{O}_{11}\text{Se}$		$\text{Al}_{10}\text{O}_{14}\text{Se}$	
Al3-Se10	2.357	Al1-O8	1.980	Al1-Se20	2.278	Al8-Se25	2.382
Al3-O7	1.738	Al6-O8	1.808	Al7-Se20	2.359	Al9-Se25	2.265
Al8-O6	1.742	Al2-Se15	2.396	Al6-O10	1.710	Al9-O15	1.818
		Al6-Se15	2.274	Al6-O15	1.790	Al9-O23	1.707
BAl_3O_6		BAl_5O_9		$\text{BAl}_7\text{O}_{12}$		$\text{BAl}_9\text{O}_{15}$	
B10-O3	1.404	Al1-O8	2.003	B20-O10	1.360	Al8-O24	1.789
Al1-O9	1.745	B15-O8	1.488	B20-O15	1.467	B25-O14	1.530
Al8-O7	1.751	B15-O7	1.357	Al1-O8	1.717	B25-O22	1.340
		B15-O12	1.357	Al6-O8	1.767	B25-O24	1.350
GaAl_3O_6		GaAl_5O_9		$\text{GaAl}_7\text{O}_{12}$		$\text{GaAl}_9\text{O}_{15}$	
Ga10-O3	1.838	Al1-O8	1.953	Ga20-O10	1.785	Al8-O24	1.789
Al1-O9	1.743	Ga15-O8	1.903	Ga20-O15	1.893	Ga25-O14	1.968
Al8-O7	1.749	Ga15-O7	1.786	Al1-O8	1.716	Ga25-O22	1.765
		Ga15-O12	1.786	Al6-O8	1.767	Ga25-O24	1.771

Table 2. Point Groups (P.G), the Obtained Frontier Molecular Orbital Energies (ϵ_H and ϵ_L), Energy Gap (E_g), Dipole Moment (μ), Polarizability (α), First Hyperpolarizability (β_0) and Second Hyperpolarizability (γ_{tot}) Values for the Considered Alumina Nanostructures

Compound	P.G	ϵ_H	ϵ_L	E_g	μ	α	β_0	γ_{tot}
Al ₄ O ₆	Td	-7.823	-3.537	4.286	0	81.66	0	21036.16
Al ₆ O ₉	C ₁	-8.144	-3.088	5.056	0.54	116.00	51.65	25586.93
Al ₈ O ₁₂	C ₁	-8.209	-3.059	5.151	0.58	155.03	35.38	33820.44
Al ₁₀ O ₁₅	C ₁	-8.304	-3.127	5.177	1.60	189.38	101.60	39885.66

ϵ_H , ϵ_L and E_g in eV; μ in Debye; α , β_0 and γ_{tot} in a.u.

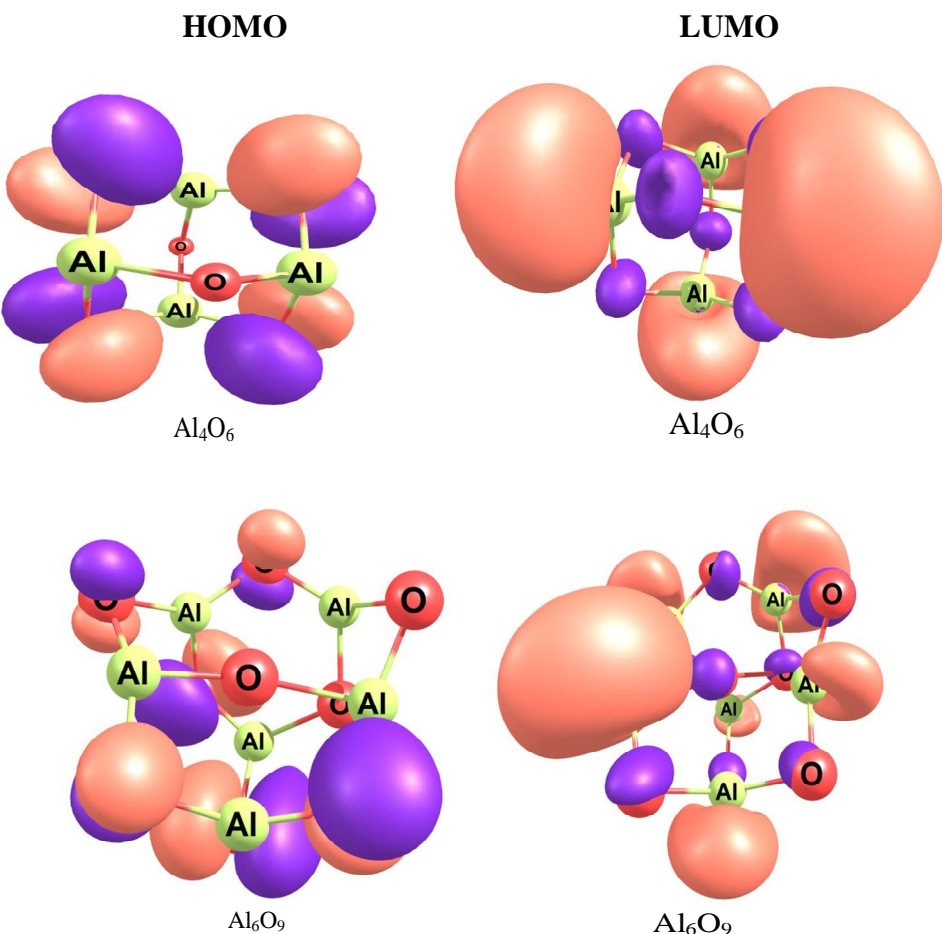


Fig. 2. Typically contour plots of HOMO and LUMO of pristine nanostructures.

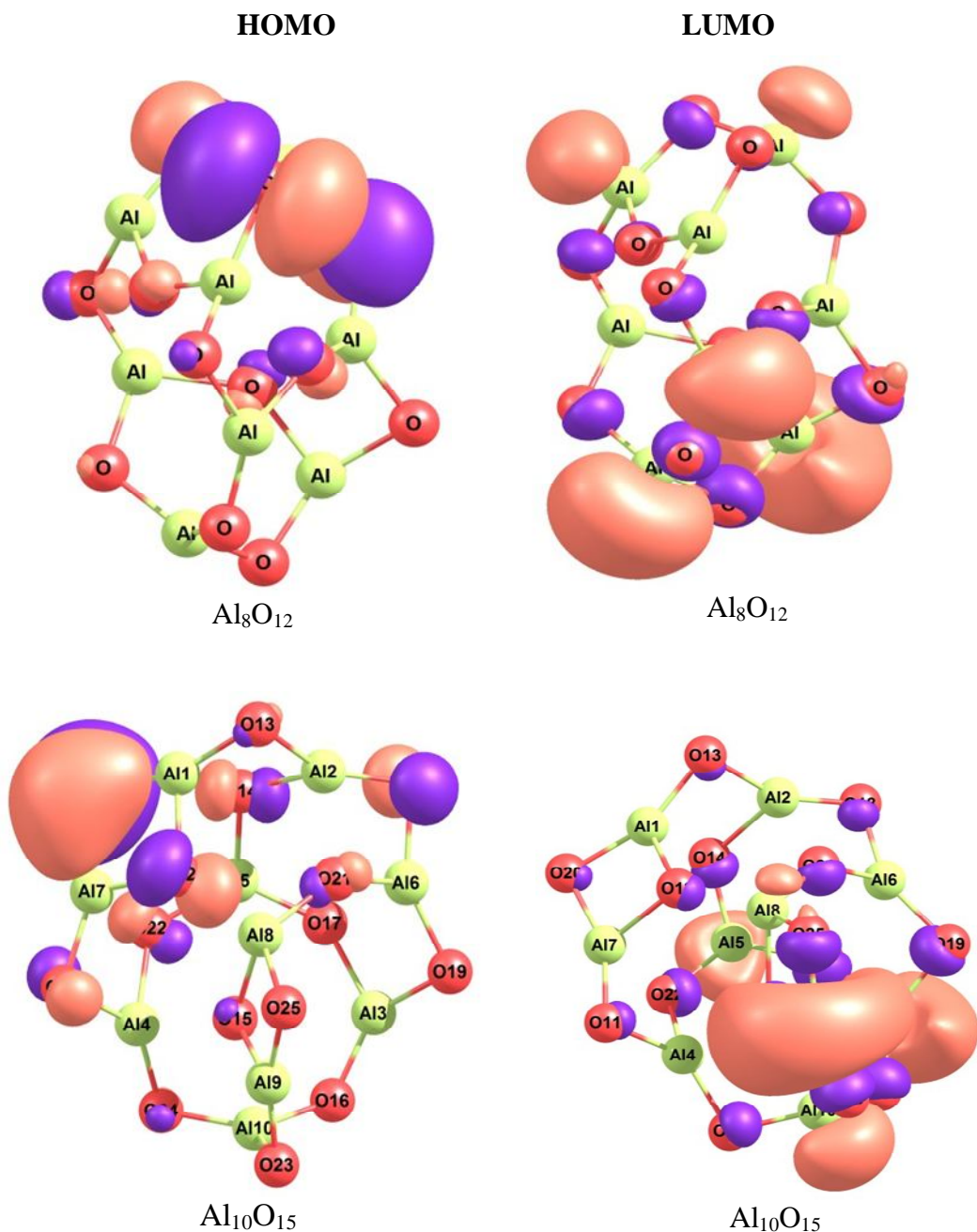


Fig. 2. Continued.

eV, taking a hint to their semiconductor character. The obtained outcomes are in agreement with the former results [20].

The graphic presentation of the HOMO-LUMO distribution of the considered alumina nanostructures is

displayed in Fig. 2. According to this figure, the HOMO is concentrated over the oxygen atoms of the nanostructures, and the LUMO are spread over the aluminum atoms. The HOMO orbital principally acts as an electron donor, and LUMO orbital mainly acts as an electron acceptor.

Moreover the calculated values of dipole moment (μ), polarizability (α), static first hyperpolarizability (β_0) and static second hyperpolarizability (γ_{tot}) are listed in Table 2.

Geometrical Characteristic and Natural Bond Orbital (NBO) of Doped Alumina Nanostructures

In this section, the structure of alumina nanostructures including different dopants are investigated and compared with each other. To this end, in Al_4O_6 nanostructure, two separate locations (Al or O) for doping are considered. In other structures, due to the asymmetry of structures, all the possible positions for doping were considered, and finally, the stable structure was selected for NLO study. In these nanostructures, an aluminum atom is substituted by an element of group III (B and Ga) and oxygen atom is replaced by an element of group VI (S and Se). The geometry of these doped alumina nanostructures optimized at the B3LYP/6-31+G(d) level of theory are displayed in Fig. 3. The point groups of doped nanostructures are listed

in Table 4. It should be mentioned that the structure of all systems is changed due to the doping process; so doping causes local deformation in the nanostructures. The achieved outcomes display that in all nanostructures, Al-S, Al-Se, and Ga-O bonds are larger than Al-O bond, indicating that the geometrical structures of the investigated systems are expanded, whereas B-O bond is smaller than Al-O bond. The significant geometrical parameters are presented in Table 1. These structural changes are anticipated to remarkably influence the electro-optical properties of the studied nanostructures.

To describe the interplay between doping atoms and alumina nanostructures, natural bond orbital (NBO) analysis has been performed, and the outcomes are given in Table 3. From Table 3, it is clarified that the S and Se atoms display negative charge, indicating that the charge transfers from nanostructures to the element of group VI, and nanostructures act as donors. According to Table 3, the charge ranges of B and Ga are from 1.221 to 1.263 and

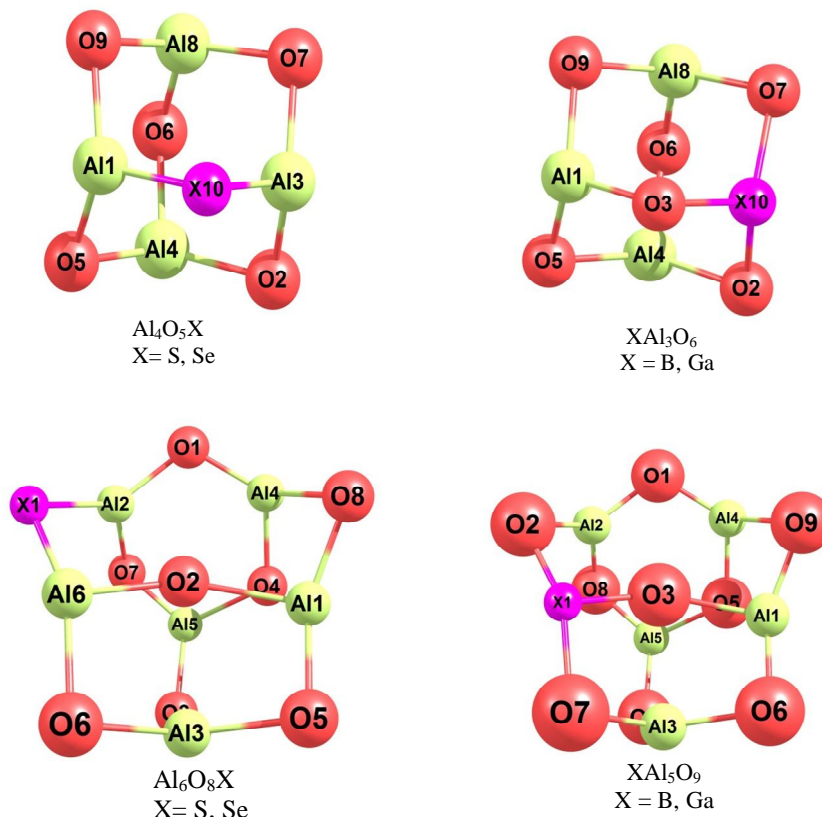


Fig. 3. Geometry of doped nanostructures.

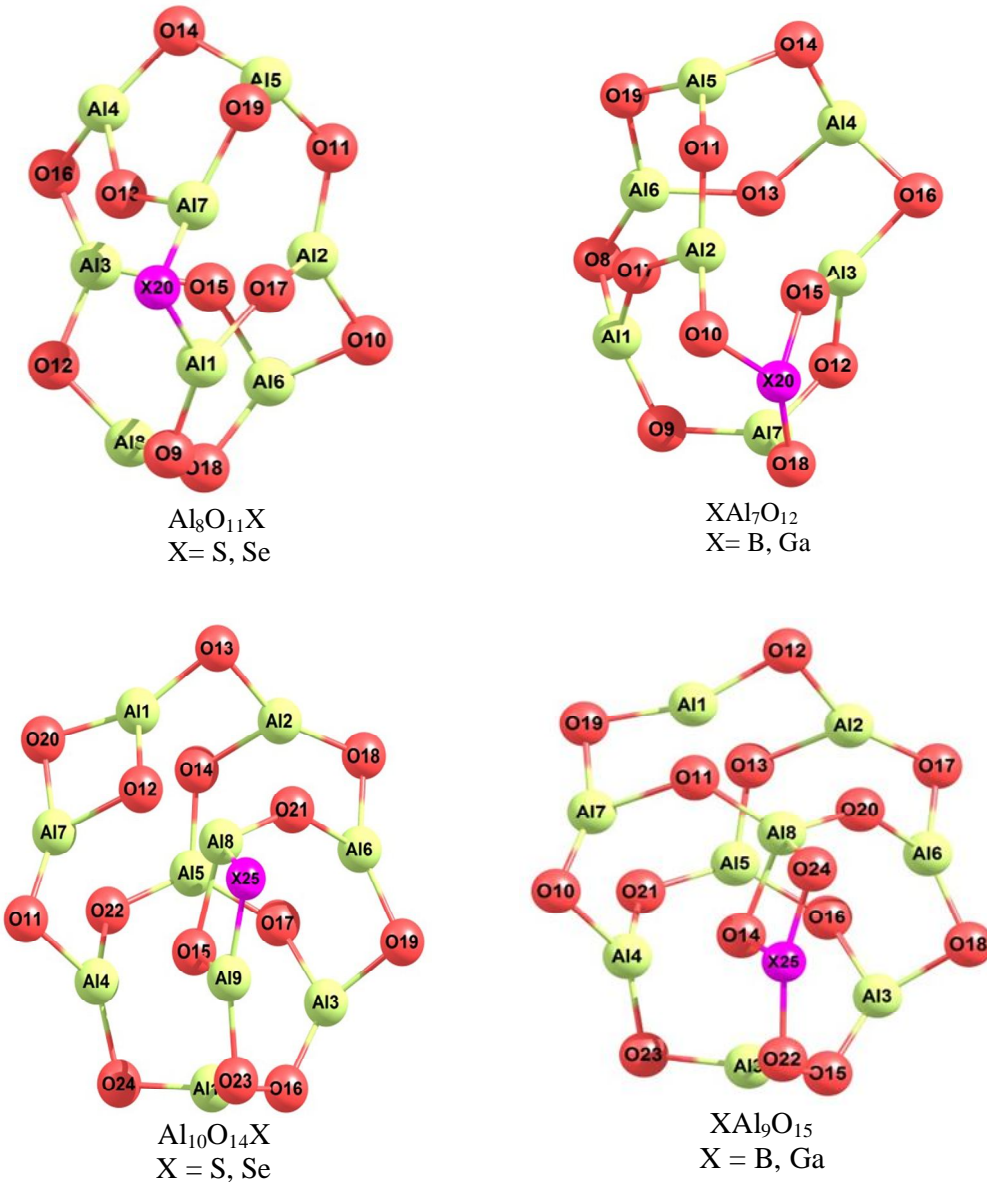


Fig. 3. Continued.

1.935 to 1.982, respectively. These illustrate that the charge transfer occurs from the element of group III to nanostructures, and nanostructures obtain negative charge from these elements, which interestingly exhibits that nanostructures act as acceptors. Hence, doped alumina nanostructures can be considered as an acceptor-donor model for NLO materials due to the enhancement of charge transfer (CT) and exhibit the large NLO response. Based on the previous studies, donor or acceptor substituents could

greatly enhance the second and third- order NLO properties [61-65].

NLO Response of Doping Alumina Nanostructures

In this part, the electronic and optical properties of the considered doped alumina nanostructures are investigated. The obtained frontier molecular orbital energies (ϵ_H and ϵ_L), the computed energy gap (Eg) values are listed in Table 4. From Table 4, doping elements of groups VI (S and Se) can

Table 3. NBO Charge of Doping Atoms

Compound	S	Se	B	Ga
Al ₄ O ₅ S	-0.918	-	-	-
Al ₄ O ₅ Se	-	-0.814	-	-
BAl ₃ O ₆	-	-	1.221	-
GaAl ₃ O ₆	-	-	-	1.935
Al ₆ O ₈ S	-0.883	-	-	-
Al ₆ O ₈ Se	-	-0.770	-	-
BAl ₅ O ₉	-	-	1.263	-
GaAl ₅ O ₉	-	-	-	1.982
Al ₈ O ₁₁ S	-0.881	-	-	-
Al ₈ O ₁₁ Se	-	-0.776	-	-
BAl ₇ O ₁₂	-	-	1.237	-
GAl ₇ O ₁₂	-	-	-	1.944
Al ₁₀ O ₁₄ S	-0.867	-	-	-
Al ₁₀ O ₁₄ Se	-	-0.754	-	-
BAl ₉ O ₁₅	-	-	1.223	-
GaAl ₉ O ₁₅	-	-	-	1.949

narrow the wide energy gap of alumina nanostructures in the range of 0.322-1.179 eV; while with doping B and Ga atoms, the energy gap of alumina nanostructures is not meaningfully modified and changes in the range of 0.042 to 0.635 eV. To explain the origin of this matter, the density of states (DOS) of pristine Al₄O₆, Al₈O₁₂ and doped nanostructures with B and Se, respectively, are plotted with gauss sum software revision 2.2 [66] and represented in Fig. 4. This figure clearly shows that the valance and conduction levels of doped nanostructures are close to those in pristine nanostructures. Also, it is clear that doping Se in nanostructures leads to increase the energy level as the newly formed HOMO reclining between the original HOMO (becoming HOMO-1 of doped systems) and LUMO of Al₈O₁₂, which is responsible for the meaningful, reduce

of the substantial E_g. In the doped B nanostructures, LUMO energy level falls down and the energy gap between HOMO and LUMO is reduced.

The doping energy (E_{dop}) required to start doping is computed under the following equation:

$$E_{dop} = E_{doped-nanostruct} + E_X - E_{nanostruct} - E_{dopant} \quad (8)$$

where E_{nanostruct} and E_{doped-nanostruct} indicate the total energy of the nanostructures and doped nanostructures. E_X is total energy for an isolated Al and O atom, and E_{dopant} displays total energy for an isolated impurity dopant (S, Se, B or Ga). The achieved E_{dop} values are summarized in Table 4. Doping energy values indicate that the doping process is associated with energy gaining except for boron doping in

Table 4. Point Groups (P.G), the Obtained Frontier Molecular Orbital Energies (ϵ_H and ϵ_L), Energy Gap (E_g), Doping Energy (E_{dop}), Dipole Moment (μ), Polarizability (α), First Hyperpolarizability (β_0) and Second Hyperpolarizability (γ_{tot}) Values for the Considered Doped Alumina Nanostructures

Compound	P.G	ϵ_H	ϵ_L	E_g	E_{dop}	μ	α	β_0	γ_{tot}
Al ₄ O ₅ S	C _{2v}	-6.909	-3.573	3.336	1.884	0.48	101.44	81.47	31214.61
Al ₄ O ₅ Se	C _{2v}	-6.547	-3.559	2.988	1.661	0.43	109.79	81.26	39399.93
BAl ₃ O ₆	C _{3v}	-7.496	-3.845	3.651	-2.482	1.11	73.32	56.65	17195.85
GaAl ₃ O ₆	C _{3v}	-7.823	-3.972	3.850	2.144	0.20	85.99	53.22	21374.95
Al ₆ O ₈ S	C ₁	-7.619	-3.126	4.493	1.850	0.73	135.89	95.56	33679.20
Al ₆ O ₈ Se	C ₁	-7.282	-3.114	4.168	1.595	0.64	143.76	87.62	39862.54
BAl ₅ O ₉	C ₁	-8.303	-3.204	5.098	-2.871	1.41	108.09	133.37	21192.14
GaAl ₅ O ₉	C ₁	-8.137	-3.460	4.677	1.795	0.51	119.37	56.65	25082.65
Al ₈ O ₁₁ S	C ₁	-7.370	-3.070	4.300	1.966	0.70	174.69	51.58	42193.24
Al ₈ O ₁₁ Se	C ₁	-7.024	-3.052	3.972	1.680	0.60	182.40	51.30	48535.54
BAl ₇ O ₁₂	C ₁	-8.433	-3.028	5.405	-3.071	0.76	146.60	68.85	28957.86
GAl ₇ O ₁₂	C ₁	-8.192	-3.535	4.657	1.886	0.62	158.88	36.24	34061.48
Al ₁₀ O ₁₄ S	C ₁	-7.910	-3.055	4.855	1.875	1.97	209.00	144.19	46636.98
Al ₁₀ O ₁₄ Se	C ₁	-7.556	-3.322	4.533	1.460	1.93	216.30	149.21	50979.00
BAl ₉ O ₁₅	C ₁	-8.536	-3.035	5.501	-3.190	1.91	181.22	147.63	34865.98
GaAl ₉ O ₁₅	C ₁	-8.332	-3.561	4.772	1.660	1.43	192.59	88.31	39502.18

Al₄O₆, Al₆O₉, Al₈O₁₂ and Al₁₀O₁₅ at which energy is released, about -2.482, -2.871, -3.071 and -3.190 eV, respectively.

The obtained dipole moment (μ), polarizability (α), static first hyperpolarizability (β_0) and static second hyperpolarizability (γ_{tot}) of the measured doped nanostructures by CAM-B3LYP method are also summarized in Table 4. From Table 4, our results display that the polarizability (α) and static first hyperpolarizability (β_0) partially and static second hyperpolarizability (γ_{tot}) meaningfully are increased due to the doping process. The effect of the size of nanostructures on its NLO response is also of our attention. Interestingly, the polarizability and

static second hyperpolarizability values of alumina nanostructures illustrate a sudden increase with enlargement of the nanostructures which is in full agreement with the results of previous studies on ZnO and CdSe clusters [67,68]. According to Table 4, the largest amount of static second hyperpolarizability is achieved by doping Se in Al₈O₁₂ and Al₁₀O₁₅ with the values 48535.54 and 50979.00 a.u, respectively. BAl₉O₁₅ and Al₁₀O₁₄Se have greatest static first hyperpolarizability with values 147.63 and 149.21 a.u, respectively. To sum up, it appears that doping process is effective to improve the NLO response of the alumina nanostructures, which will be beneficial for advancement the multifield applications of the inorganic alumina

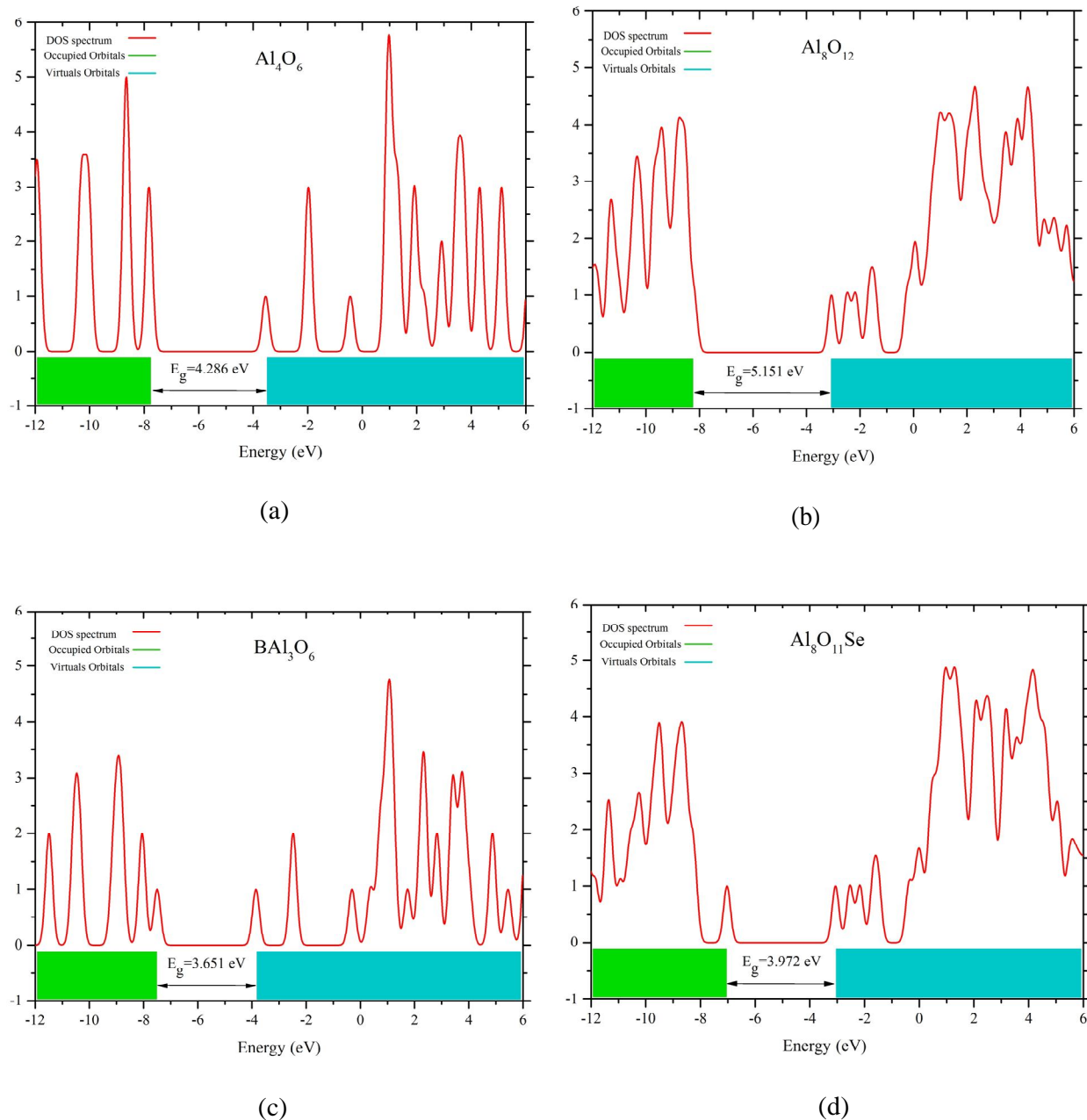


Fig. 4. Density of states (DOS) of Al_4O_6 (a), Al_8O_{12} (b), BaAl_3O_6 (c), and $\text{Al}_8\text{O}_{11}\text{Se}$ (d) of alumina nanostructures.

nanostructures in electronic nanodevices and high performance NLO nanomaterials.

CONCLUSIONS

In this study, we have investigated nonlinear optical

features of alumina nanostructures with the groups III and VI dopants. The NBO analysis displays that these nanostructures act as donors as well as acceptors and lead to charge transfer between nanostructures and doping atom. DOS spectrum reveals that the valance and conduction levels of doped nanostructures are close to those in pristine

nanostructures. In other words, it can be seen that the decrease of energy gap can be due to production a new high energy level to offer a new HOMO in the original gap of alumina nanostructures. Furthermore, doping of III and VI groups in the considered nanostructures partially increases polarizability and static first hyperpolarizability and significantly static second hyperpolarizability. Our data illustrated that polarizability and static second hyperpolarizability are increased with enlargement of the nanostructures. In particular, doping the element of groups III and VI can increase the NLO properties of the alumina nanostructures, which may have potential applications in nanoelectronics.

ACKNOWLEDGMENTS

The author gratefully acknowledges the research council of Arak University for financial support (Grant No. 93.12222).

SUPPORTING INFORMATION

The optimized coordinates of all studied systems at B3LYP/6-31+G(d) computational level.

REFERENCES

- [1] Goto, M.; Murakami, J.; Tai, Y.; Igarashi, K.; Tanemura, S.; Kusunoki, M., Generation of novel aluminum nano balls. *Jpn. J. Appl. Phys.* **1998**, *37*, (12B):L1537. DOI:10.1143/JJAP.37.L1537.
- [2] Janiak, C., Metallocene catalysts for olefin polymerization. In: *Metallocenes: Synthesis Reactivity Applications*. **1998**, pp. 547-623.
- [3] Kaminsky, W., New polymers by metallocene catalysis. *Macromol. Chem. Phys.* **1996**, *197*, 3907-3945. DOI: 10.1002/macp.1996.021971201.
- [4] Chopra, N. G.; Luyken, R.; Cherrey, K.; Crespi, V. H.; Cohen, M. L.; Louie, S. G.; Zettl, A., Boron nitride nanotubes. *Science* **1995**, *269*, 966-967. DOI: 10.1126/science.269.5226.966.
- [5] Nakamura, H.; Matsui, Y., Silica gel nanotubes obtained by the sol-gel method. *J. Am. Chem. Soc.* **1995**, *117*, 2651-2652. DOI: 10.1021/ja00114a031.
- [6] Pu, L.; Bao, X.; Zou, J.; Feng, D., Individual alumina nanotubes. *Angew. Chem. Int. Ed.* **2001**, *40*, 1490-1493. DOI: 10.1002/1521-3773(20010417)40:8<1490:AID-ANIE1490>3.0.CO;2-K.
- [7] Linnolahti, M.; Pakkanen, T. A., Molecular structures of alumina nanoballs and nanotubes: A theoretical study. *Inorg. Chem.* **2004**, *43*, 1184-1189. DOI: 10.1021/ic0349353.
- [8] Zhong, M. -M.; Kuang, X. -Y.; Wang, H. -Q.; Li, H. -F.; Zhao, Y. -R., Density functional study of the structural and electronic properties of tetra-aluminum oxide ($3 \leq n \leq 8$, $\lambda = 0, -1$) clusters. *Mol. Phys.* **2011**, *109*, 603-612. DOI: 10.1080/00268976.2010.542777.
- [9] Fernández, E.; Balbas, L.; Borstel, G.; Soler, J., First principles calculation of the geometric and electronic structure of $(\text{Al}_2\text{O}_3)_n(\text{O}_x)$ clusters with $n < 15$ and $x = 0, 1, 2$. *Thin Solid Films* **2003**, *428*, 206-210. DOI: 10.1016/S0040-6090(02)01264-6.
- [10] Fernandez, E.; Borstel, G.; Soler, J.; Balbas, L., Study of $(\text{Al}_2\text{O}_3)_n(\text{O}_x)$ clusters with $n = 16$ and $x = 0, 1, 2$ from first principles calculations. *E. P. J. D* **2003**, *24*, 245-248. DOI: 10.1140/epjd/e2003-00151-4.
- [11] Desai, S. R.; Wu, H.; Rohlfing, C. M.; Wang, L. -S., A study of the structure and bonding of small aluminum oxide clusters by photoelectron spectroscopy: Al_xO_y ($x = 1-2$, $y = 1-5$). *J. Chem. Phys.* **1997**, *106*, 1309-1317. DOI: 10.1063/1.474085.
- [12] Chertikhin, G.; Serebreenikov, L.; Shevelkov, V., IR and Raman spectra of Al_2O_2 isomers in argon matrices. *Russ. J. Phys. Chem.* **1991**, *65*, 565-567.
- [13] Sarker, M. I. M.; Kim, C. -S.; Choi, C. H., Ground and excited states of Al_2O_2 and its anion. *Chem. Phys. lett.* **2005**, *411*, 297-301. DOI: 10.1016/j.cplett.2005.05.127.
- [14] Chang, C.; Patzer, A.; Sedlmayr, E.; Steinke, T.; Sülzle, D., Electronic structure investigation of the Al_4O_4 molecule. *Chem. Phys. lett.* **2000**, *324*, 108-114. DOI: 10.1016/S0009-2614(00)00579-0.
- [15] Zheng, X.; Zhang, Y.; Huang, S.; Liu, H.; Wang, P.; Tian, H., DFT study of structural, electronic and vibrational properties of pure $(\text{Al}_2\text{O}_3)_n$ ($n = 9, 10, 12, 15$) and Ni-doped $(\text{Al}_2\text{O}_3)_n$ ($n = 9, 10$) clusters. *Appl. Surf. Sci.* **2011**, *257*, 6410-6417. DOI: 10.1016/j.apsusc.2011.02.009.

- [16] Gu, Y.; Xu, N.; Lin, M.; Tan, K., Structures, stabilities and properties of hollow $(\text{Al}_2\text{O}_3)_n$ clusters ($n = 10, 12, 16, 18, 24$ and 33): Studied with density functional theory. *Comput. Theor. Chem.* **2015**, *1063*, 29-34. DOI: 10.1016/j.comptc.2015.03.027.
- [17] Li, R.; Cheng, L., Structural determination of $(\text{Al}_2\text{O}_3)_n$ ($n = 1-7$) clusters based on density functional calculation. *Comput. Theor. Chem.* **2012**, *996*, 125-131. DOI: 10.1016/j.comptc.2012.07.027.
- [18] Zhang, Q.; Cheng, L., Structural determination of $(\text{Al}_2\text{O}_3)_n$ ($n = 1-15$) clusters based on graphic processing unit. *J. Chem. Inf. Model.* **2015**, *55*, 1012-1020. DOI: 10.1021/acs.jcim.5b00069.
- [19] Sun, J.; Lu, W. -C.; Zhang, W.; Zhao, L. -Z.; Li, Z. -S.; Sun, C. -C., Theoretical study on $(\text{Al}_2\text{O}_3)_n$ ($n = 1-10$ and 30) fullerenes and H_2 adsorption properties. *Inorg. Chem.* **2008**, *47*, 2274-2279. DOI: 10.1021/ic7011364.
- [20] Rahane, A. B.; Deshpande, M. D.; Kumar, V., Structural and electronic properties of $(\text{Al}_2\text{O}_3)_n$ clusters with $n = 1-10$ from first principles calculations. *J. Phys. Chem. C* **2011**, *115*, 18111-18121. DOI: 10.1021/jp2050614.
- [21] Moloney, J. V., Nonlinear optical materials. vol 101. Springer Science & Business Media. **1998**.
- [22] Xu, H. -L.; Li, Z. -R.; Su, Z. -M.; Muhammad, S.; Gu, F. L.; Harigaya, K., Knot-isomers of Möbius cyclacene: how does the number of knots influence the structure and first hyperpolarizability? *J. Phys. Chem. C* **2009**, *113*, 15380-15383. DOI: 10.1021/jp901358f.
- [23] Nakano, M.; Fujita, H.; Takahata, M.; Yamaguchi, K., Theoretical study on second hyperpolarizabilities of phenylacetylene dendrimer: toward an understanding of structure-property relation in NLO responses of fractal antenna dendrimers. *J. Am. Chem. Soc.* **2002**, *124*, 9648-9655. DOI: 10.1021/ja0115969.
- [24] Xu, H. -L.; Li, Z. -R.; Wang, F. -F.; Wu, D.; Harigaya, K.; Gu, F. L., What is the shape effect on the (hyper) polarizabilities? A comparison study on the Möbius, normal cyclacene, and linear nitrogen-substituted strip polyacenes. *Chem. Phys. lett.* **2008**, *454*, 323-326. DOI: 10.1016/j.cplett.2008.02.035.
- [25] Matsuzawa, N.; Seto, J. E.; Dixon, D. A., Density functional theory predictions of second-order hyperpolarizabilities of metallocenes. *J. Phys. Chem. A* **1997**, *101*, 9391-9398. DOI: 10.1021/jp952465v.
- [26] Matsuzawa, N.; Ata, M.; Dixon, D. A., Density functional theory prediction of the second-order hyperpolarizability of metalloporphines. *J. Phys. Chem.* **1995**, *99*, 7698-7706. DOI: 10.1021/j100019a058.
- [27] Matsuzawa, N.; Dixon, D. A., Theoretical study of the conformation and second-order hyperpolarizability of substituted phenylpolyacetylenes. *J. Phys. Chem.* **1994**, *98*, 11669-11676. DOI: 10.1021/j100096a008.
- [28] Coe, B. J., Switchable nonlinear optical metallocromophores with pyridinium electron acceptor groups. *Acc. Chem. Res.* **2006**, *39*, 383-393. DOI: 10.1021/ar050225k.
- [29] Coe, B. J.; Foxon, S. P.; Harper, E. C.; Raftery, J.; Shaw, R.; Swanson, C. A.; Asselberghs, I.; Clays, K.; Brunschwig, B. S.; Fitch, A. G., Nonlinear optical and related properties of iron(II) pentacyanide complexes with quaternary nitrogen electron acceptor units. *Inorg. Chem.* **2009**, *48*, 1370-1379. DOI: 10.1021/ic801224u.
- [30] Janjua, M. R. S. A.; Liu, C. -G.; Guan, W.; Zhuang, J.; Muhammad, S.; Yan, L. -K.; Su, Z. -M., Prediction of remarkably large second-order nonlinear optical properties of organoimido-substituted hexamolybdates. *J. Phys. Chem. A* **2009**, *113*, 3576-3587. DOI: 10.1021/jp808707q.
- [31] Lee, S. H.; Park, J. R.; Jeong, M. Y.; Kim, H. M.; Li, S.; Song, J.; Ham, S.; Jeon, S. J.; Cho, B. R., First hyperpolarizabilities of 1,3,5-tricyanobenzene derivatives: origin of larger β values for the octupoles than for the dipoles. *Chem. Phys. Chem.* **2006**, *7*, 206-212. DOI: 10.1002/cphc.200500274.
- [32] Meyers, F.; Marder, S.; Pierce, B.; Bredas, J., Electric field modulated nonlinear optical properties of donor-acceptor polyenes: sum-over-states investigation of the relationship between molecular polarizabilities (alpha, beta and gamma) and bond length alternation. *J. Am. Chem. Soc.* **1994**, *116*, 10703-10714. DOI: 10.1021/ja00102a040.
- [33] Yang, J. -S.; Liau, K. -L.; Li, C. -Y.; Chen, M. -Y., Meta conjugation effect on the torsional motion of

- aminostilbenes in the photoinduced intramolecular charge-transfer state. *J. Am. Chem. Soc.* **2007**, *129*, 13183-13192. DOI: 10.1021/ja0741022.
- [34] Kanis, D. R.; Ratner, M. A.; Marks, T. J., Design and construction of molecular assemblies with large second-order optical nonlinearities. Quantum chemical aspects. *Chem. Rev.* **1994**, *94*, 195-242. DOI: 10.1021/cr00025a007.
- [35] Li, Z. -J.; Wang, F. -F.; Li, Z. -R.; Xu, H. -L.; Huang, X. -R.; Wu, D.; Chen, W.; Yu, G. -T.; Gu, F. L.; Aoki, Y., Large static first and second hyperpolarizabilities dominated by excess electron transition for radical Ion pair salts M^{2+} TCNQ-($M = Li, Na, K$). *Phys. Chem. Chem. Phys.* **2009**, *11*, 402-408. DOI: 10.1039/B809161G
- [36] Liu, Z. -B.; Zhou, Z. -J.; Li, Y.; Li, Z. -R.; Wang, R.; Li, Q. -Z.; Li, Y.; Jia, F. -Y.; Wang, Y. -F.; Li, Z. -J., Push-pull electron effects of the complexant in a Li atom doped molecule with electride character: a new strategy to enhance the first hyperpolarizability. *Phys. Chem. Chem. Phys.* **2010**, *12*, 10562-10568. DOI: 10.1039/C004262E
- [37] Wang, F. -F.; Li, Z. -R.; Wu, D.; Wang, B. -Q.; Li, Y.; Li, Z. -J.; Chen, W.; Yu, G. -T.; Gu, F. L.; Aoki, Y., Structures and considerable static first hyperpolarizabilities: New organic alkalides ($M^+ @ n$ 6adz) $M''(M, M' = Li, Na, K; n = 2, 3)$ with Cation Inside and Anion Outside of the Cage Complexants. *J. Phys. Chem. B* **2008**, *112*, 1090-1094. DOI: 10.1021/jp076790h.
- [38] Xu, H. -L.; Li, Z. -R.; Wu, D.; Ma, F.; Li, Z. -J.; Gu, F. L., Lithiation and Li-doped effects of [5] cyclacene on the static first hyperpolarizability. *J. Phys. Chem. C* **2009**, *113*, 4984-4986. DOI: 10.1021/jp806864w.
- [39] Fainman, Y.; Ma, J.; Lee, S. H., Non-linear optical materials and applications. *Mater. Sci. Rep.* **1993**, *9*, 53-139. DOI: 10.1016/0920-2307(93)90008-3.
- [40] Sugawara, M.; Ebe, H.; Hatori, N.; Ishida, M.; Arakawa, Y.; Akiyama, T.; Otsubo, K.; Nakata, Y., Theory of optical signal amplification and processing by quantum-dot semiconductor optical amplifiers. *Phys. Rev. B* **2004**, *69*, 235332. DOI: 10.1103/PhysRevB.69.235332.
- [41] Demyk, K.; Van Heijnsbergen, D.; Von Helden, G.; Meijer, G., Experimental study of gas phase titanium and aluminum oxide clusters. *Astronom. and Astrophys.* **2004**, *420*, 547-552. DOI: 10.1051/0004-6361:20034117.
- [42] Sierka, M., Synergy between theory and experiment in structure resolution of low-dimensional oxides. *Prog. Surf. Sci.* **2010**, *85*, 398-434. DOI: 10.1016/j.progsurf.2010.07.004.
- [43] Becke, A. D., Density-functional thermochemistry. III. The role of exact exchange. *J. Chem. Phys.* **1993**, *98*, 5648-5652. DOI: 10.1063/1.464913.
- [44] Parr, R. G.; Yang, R. G. P. W., Density-functional theory of atoms and molecules. Oxford university press. **1989**.
- [45] Ahmadi, A.; Beheshtian, J.; Hadipour, N. L., Interaction of NH_3 with aluminum nitride nanotube: electrostatic vs. covalent. *Physica. E* **2011**, *43*, 1717-1719. DOI: 10.1016/j.physe.2011.05.029.
- [46] Shakerzadeh, E., A theoretical study on pristine and doped germanium carbide nanoclusters. *J. Mater. Sci. Mater. Electron.* **2014**, *25*, 4193-4199. DOI: 10.1007/s10854-014-2148-z.
- [47] Reed, A. E.; Weinstock, R. B.; Weinhold, F., Natural population analysis. *J. Chem. Phys.* **1985**, *83*, 735-746. DOI: 10.1063/1.449486.
- [48] Yanai, T.; Tew, D. P.; Handy, N. C., A new hybrid exchange-correlation functional using the Coulomb-attenuating method (CAM-B3LYP). *Chem. Phys. lett.* **2004**, *393*, 51-57. DOI: 10.1016/j.cplett.2004.06.011.
- [49] Tawada, Y.; Tsuneda, T.; Yanagisawa, S.; Yanai, T.; Hirao, K., A long-range-corrected time-dependent density functional theory. *J. Chem. Phys.* **2004**, *120*, 8425-8433. DOI: 10.1063/1.1688752.
- [50] Alparone, A., Response electric properties of α -helix polyglycines: A CAM-B3LYP DFT investigation. *Chem. Phys. lett.* **2013**, *563*:88-92. DOI: 10.1016/j.cplett.2013.01.062.
- [51] Peach, M. J.; Helgaker, T.; Sałek, P.; Keal, T. W.; Lutnæs, O. B.; Tozer, D. J.; Handy, N. C., Assessment of a Coulomb-attenuated exchange-correlation energy functional. *Phys. Chem. Chem. Phys.* **2006**, *8*, 558-562. DOI: 10.1039/B511865D.
- [52] Jacquemin, D.; Perpète, E. A.; Scalmani, G.; Frisch, M. J.; Kobayashi, R.; Adamo, C., First

- hyperpolarizability of polymethineimine with long-range corrected functionals. *J. Chem. Phys.* **2007**, *126*, 191108. DOI: 10.1063/1.2741246.
- [53] Limacher, P. A.; Mikkelsen, K. V.; Lüthi, H. P., On the accurate calculation of polarizabilities and second hyperpolarizabilities of polyacetylene oligomer chains using the CAM-B3LYP density functional. *J. Chem. Phys.* **2009**, *130*, 194114. DOI: 10.1063/1.3139023.
- [54] Suponitsky, K. Y.; Tafur, S.; Masunov, A. E., Applicability of hybrid density functional theory methods to calculation of molecular hyperpolarizability. *J. Chem. Phys.* **2008**, *129*, 044109. DOI: 10.1063/1.2936121.
- [55] Song, Y. -D.; Wu, L. -M.; Chen, Q. -L.; Liu, F. -K.; Tang, X. -W., How lithium atoms affect the first hyperpolarizability of BN edge-doped graphene. *J. Mol. Model.* **2016**, *22*, 1-8. DOI: 10.1007/s00894-015-2899-3.
- [56] Song, H.; Zhang, M.; Yu, H.; Wang, C.; Zou, H.; Ma, N.; Qiu, Y., The Li-substituted effect on the geometries and second-order nonlinear optical properties of indeno [1,2-b] fluorene. *Comput. Theor. Chem.* **2014**, *1031*, 7-12
- [57] Frisch, M.; Trucks, G.; Schlegel, H.; Scuseria, G.; Robb, M.; Cheeseman, J.; Montgomery Jr, J.; Vreven, T.; Kudin, K.; Burant, J., Pittsburgh PA, Pople JA (2009) Gaussian 09, revision A02. *Gaussian Inc, Wallingford*. DOI: 10.1016/j.comptc.2014.01.005.
- [58] Bonin, K. D.; Kresin, V. V., Electric-dipole polarizabilities of atoms, molecules, and clusters. *World Scientific*. **1997**.
- [59] McLean, A.; Yoshimine, M., Theory of molecular polarizabilities. *J. Chem. Phys.* **1967**, *47*, 1927-1935. DOI: 10.1063/1.1712220.
- [60] Buckingham, A.; Orr, B., Molecular hyperpolarisabilities. *Q. Rev. Chem. Soc.* **1967**, *21*, 195-212. DOI: 10.1039/QR9672100195.
- [61] Zhang, M.; Li, G.; Li, L., Graphene nanoribbons generate a strong third-order nonlinear optical response upon intercalating hexagonal boron nitride. *J. Mater. Chem. C* **2014**, *2*, 1482-1488. DOI: 10.1039/c3tc31847h.
- [62] Xu, H. -L.; Li, Z. -R.; Wu, D.; Wang, B. -Q.; Li, Y.; Gu, F. L.; Aoki, Y., Structures and large NLO responses of new electrides: Li-doped fluorocarbon chain. *J. Am. Chem. Soc.* **2007**, *129*, 2967-2970. DOI: 10.1021/ja068038k.
- [63] Li, X. -Q.; Wang, C. -H.; Zhang, M. -Y.; Zou, H. -Y.; Ma, N. -N.; Qiu, Y. -Q., Tuning second-order nonlinear optical properties of the two-dimensional benzene/carborane compounds with phenyl carbazoles: Substituent effect and redox switch. *J. Organomet. Chem.* **2014**, *749*:327-334. DOI: 10.1016/j.jorgancem.2013.10.018.
- [64] Nakano, M.; Yamada, S.; Yamaguchi, K., Analysis of spatial contribution to the second hyperpolarizabilities of π -conjugated systems involving sulfur atoms. *J. Phys. Chem. A* **1999**, *103*, 3103-3109. DOI: 10.1021/jp984665n.
- [65] Meyers, F.; Marder, S. R.; Pierce, B. M.; Bredas, J. L., Electric field modulated nonlinear optical properties of donor-acceptor polyenes: Sum-over-states investigation of the relationship between molecular polarizabilities (alpha, beta, and gamma) and bond length alternation. *J. Am. Chem. Soc.* **1994**, *116*, 10703-10714. DOI: 10.1021/ja00102a040.
- [66] O'boyle, N. M.; Tenderholt, A. L.; Langner, K. M., Cclib: a library for package-independent computational chemistry algorithms. *J. Comput. Chem.* **2008**, *29*, 839-845. DOI: 10.1002/jcc.20823.
- [67] Li, L.; Zhou, Z.; Wang, X.; Huang, W.; He, Y.; Yang, M., First-principles study of static polarizability, first and second hyperpolarizabilities of small-sized ZnO clusters. *Phys. Chem. Chem. Phys.* **2008**, *10*, 6829-6835. DOI: 10.1039/B811610E
- [68] Sen, S.; Chakrabarti, S., Frequency-dependent nonlinear optical properties of CdSe clusters. *Phys. Rev. B* **2006**, *74*, 205435. DOI: 10.1103/PhysRevB.74.205435.